



Phylogenetic relationship analysis of leafhopper subfamily Iassinae (Hemiptera: Cicadellidae) based on low-coverage whole-genome data

Xiaozhen Lu^{1,*}, Jikai Lu^{1,*}, Yunfei Wu^{1,2}, Meishu Guo¹, Guy Smagghe^{1,3,4}, Renhuai Dai¹

¹ Institute of Entomology, Guizhou University, The Provincial Key Laboratory for Agricultural Pest Management Mountainous Region, Guiyang, Guizhou 550025, China

² College of Biology and Food Engineering, Chuzhou University, Chuzhou, Anhui, China

³ Department of Plants and Crops, Ghent University, Ghent 9000, Belgium

⁴ Department of Biology, Vrije Universiteit Brussels (VUB), 1050 Brussels, Belgium

* These authors contributed equally to the work.

<https://zoobank.org/509AE662-7EE2-4D49-9F20-D0E379B03B3E>

Corresponding author: Ren-huai Dai (rh dai@gzu.edu.cn)

Received 27 September 2024

Accepted 21 December 2024

Published 25 February 2025

Academic Editors André Nel, Marianna Simões

Citation: Lu X, Lu J, Wu F, Guo S, Smagghe G, Dai R (2025) Phylogenetic relationship analysis of leafhopper subfamily Iassinae (Hemiptera: Cicadellidae) based on low-coverage whole-genome data. *Arthropod Systematics & Phylogeny* 83: 31–41. <https://doi.org/10.3897/asp.83.e142332>

Abstract

Iassinae, a widely distributed group of herbivorous pest insects, is a subfamily of Cicadellidae. Previous studies on the phylogeny of Iassinae were mostly based on morphological characteristics, mitochondrial genomes, and molecular fragments (H3, 28S, and 12S), and their phylogenetic relationships were controversial. To better understand Iassinae, we analyzed the phylogenetic relationships among four genera in Iassinae with use of thousands of universal single-copy orthologs and ultraconserved elements extracted from 25 newly sequenced low-coverage whole genome data. Both marker sets provided consistent results across the maximum likelihood and coalescent-based species tree approaches. The phylogenetic results showed that the two genera *Batracomorphus* and *Trocnadella* were monophyletic groups, and *Krisna* a paraphyletic group. For the genus *Gessius*, we could not explain whether it is monophyletic or paraphyletic since only one species was involved. In this study, the phylogenetic relationship with use of universal single-copy orthologs and ultraconserved elements was stable, and all results supported that *Batracomorphus* is a sister group of *Trocnadella*, and that *Gessius* and *Krisna* possess a sister relationship. In addition, the divergence time showed that the divergence of *Batracomorphus*, *Trocnadella*, *Krisna* and *Gessius* began at approximately 49–72 Mya, 33–57 Mya, 51–78 Mya and 17–36 Mya, respectively. These results will help us to understand the phylogeny and evolutionary relationship of Iassinae.

Key words

Iassinae; systematics; ultraconserved element; universal single-copy ortholog; divergence time

1. Introduction

Leafhoppers (Cicadellidae) compose the largest family in the order of Hemiptera, comprising one of the most diverse groups of plant-feeding insects, with over 22,000

described species (Dai et al. 2015; Wang et al. 2017; Gonçalves et al. 2017; Domahovski et al. 2019). Iassinae is one of the 25 subfamilies of Cicadellidae with 12 tribes

over 160 genera, and more than 2,200 species known to date (Domahovski et al. 2023). Most of its tribes and genera are only found in one continent or region (Krishnankutty et al. 2016). Although most species in this subfamily are arboreal and many live on specific woody plants, the host relationships of most known species remain unknown (Krishnankutty et al. 2016; Wang et al. 2020). Iassinae insects can directly harm plants through their piercing-sucking mouthparts and can also serve as vectors for viruses, causing indirect harm to plants, and this results in slow growth or even death of the plants (Yang et al. 2023). Previous phylogenetic studies of the Iassinae were mostly based on morphological characteristics (Blocker 1979; Dietrich et al. 2001; Dietrich 2005), mitochondrial genomes (Wang et al. 2020; Yang et al. 2023), and molecular fragments (H3, 28S and 12S) (Krishnankutty et al. 2016), and the use of low coverage whole genome sequencing (LCWGS) data may help to better understand the phylogenetic relationships among the members of Iassinae.

Early phylogenetic analysis of the entire superfamily Membracoidea based on morphology restored Iassinae to monophyletic (Dietrich 1999), and then Dietrich et al. (2017) confirmed this view based on molecular data. However, Hu et al. (2022) obtained 2,395 universal single-copy orthologs (USCOs) based on transcriptome data to construct the phylogenetic relationship of Membracoidea and restored the Cicadellidae to paraphyletic, indicating that Iassinae is polyphyletic. Krishnankutty et al. (2016) analyzed 91 discrete morphological characteristics and DNA sequence data from nuclear 28S rDNA, histone H3 gene and mitochondrial 12S rDNA to study the phylogenetic relationship of the main lineages of Iassinae, and the results showed that *Batracomorphus*, *Gessius* and *Krisna* were monophyletic, while Yang et al. (2023) found that *Krisna* was paraphyletic by mitochondrial genome data. Therefore, the phylogenetic relationship of Iassinae is worthy of further investigation.

In recent years, next-generation sequencing (NGS) has greatly improved the collection of homologous genes for systematic genomics research and promoted the development of biological systematics (Young and Gillung 2020; Williams et al. 2020). Transcriptome sequencing (Lei and Dong 2016; Branstetter et al. 2021) and hybridization enrichment (Dietrich et al. 2017; Peters et al. 2017; Ma et al. 2023) were used to generate a large-scale phylogenetic dataset for phylogenetic reconstruction and provided strong support for phylogenetic relationships between species (Kapli et al. 2020). However, transcriptome sequencing requires higher freshness of muscle tissue, the success rate of locus capture is low and the generation of non-gap missing data is high, which often makes it impossible to obtain high-quality RNA (Ozsolak and Milos 2011; Bossert et al. 2019), the cost of hybridization enrichment is high and requires at least some 'model' DNA sequences that can be used to design probes targeting the target site (Lemmon et al. 2012; Zhang et al. 2022). LCWGS largely solves the shortcomings of the previous two methods, and can

also extract multiple different marker types from each LCWGS data, which has significant advantages over transcriptome sequencing and hybridization enrichment (Lemmon and Lemmon 2013; Allen et al. 2017; Zhang et al. 2019; Zhang et al. 2022).

LCWGS data have been widely used to obtain hundreds of genetic markers to reconstruct the phylogenetic relationship of insects. Zhang et al. (2019) extracted important phylogenetic gene markers, USCOs and ultraconserved elements (UCEs) from LCWGS data and used two molecular markers to study the phylogenetic relationship of Collembola. Hence, the problem with which Leo (2019) studied the phylogenetic relationship of Collembola was solved, and the feasibility of applying LCWGS data to evolutionary systematics was verified. Zhang et al. (2022) clarified the phylogenetic relationship between *Homalictus* and *Rostrohalictus* in Halictini using LCWGS data and proved that *Homalictus* and *Rostrohalictus* belong to a subgenus of *Lasioglossum*, indicating that molecular markers of USCOs and UCEs can help to classify populations with confused taxonomic status.

In this study, we extracted the phylogenetic gene markers USCOs and UCEs from the newly sequenced 25 LCWGS data, used two molecular markers to study the phylogenetic relationship of Iassinae, and elucidated the phylogenetic relationship of several genera in Iassinae. We estimated the divergence time within the Iassinae based on the inferred topology. We believe that our new molecular data provide a new perspective on the taxonomy, population genetics and evolution of leafhoppers.

2. Material and methods

2.1. Taxon sampling and sequencing

This study constructed phylogenetic trees using 25 species from the subfamily Iassinae as the ingroup, and *Tinobregmus viridescens* and *Ponana quadralaba* as the outgroup (these two groups were downloaded from NCBI; the accession numbers are SRR2496641 and SRR1821957). Specimen identification was completed by LJK through morphological characteristics. After the identification, the genital number was stored in a PCR tube containing glycerol, and the remaining tissues were used for total DNA extraction. Our voucher specimens were stored at the Institute of Entomology, Guizhou University, Guiyang, P. R. China.

Qubit precise quantitative detection and agarose electrophoresis were performed to assess the DNA quality. The concentration of our samples was between 28.83 ng/ μ L and 230.5 ng/ μ L by Qubit detection, and the total amount was between 1,614 ng and 13,138 ng. The target band of electrophoresis detection was located at about 10,000 bp, and all samples met the standard of resequencing and database construction. The total genomic DNA of

25 species of Iassinae was re-sequenced using the Illumina HiSeq 6000 sequencing platform (Beijing Berry and Kang Biotechnology) to obtain 150 bp double-end sequencing data. The clean data reported in this paper have been deposited in the Genome Sequence Archive (Chen et al. 2021) in National Genomics Data Center (CNCB-NGDC Members and Partners 2022), China National Center for Bioinformation / Beijing Institute of Genomics, Chinese Academy of Sciences (GSA: CRA016669) that are publicly accessible at <https://ngdc.cnbc.ac.cn/gsa>.

2.2. Genome assembly

Using the rapid-assembly pipeline PLWS v1.0.6 to assemble all sequenced genomes (<https://github.com/xt-mtd/PLWS>; Zhang et al. 2019). We used the `clumpify.sh` script in BBTools-38.91 software for quality control to delete duplicate data (Bushnell 2014), and then the `bbduk.sh` component of the software for quality control to prune data smaller than Q15 and retain data larger than Q20. When the data were filtered and the length of the retained data was less than 15 bp, the entire sequence needed to be removed; it was also necessary to remove multiple N-repeated data. The `bbnorm.sh` component in BBTools v.38.91 software was used to reduce the abundance of data and reduce the average depth of high coverage data for downstream analysis (Chen et al. 2018).

The quality-controlled genomic data were assembled using Minia v.3.2.4 software to construct the initial contigs, and the contigs of each locus were grouped to reach the level of contigs (Chikhi and Rizk 2013). Redundans v.0.13c software was then used to remove redundant contigs (Pryszcz and Gabaldon 2016). We used Minimap v.2.9 software to generate sequence-extended mapping files, and then SAMtools v.1.7 to convert the mapping files into sorted and indexed BAM format (Li et al. 2009; Li 2018). BESST.2.2 software and SOAPdenovo2 component in GapCloser.1.12 software were employed to extend contigs and fill gaps (Luo et al. 2012; Sahlin et al. 2014). Finally, we only kept sequences longer than 1,000 bp.

2.3. Matrix generation

For matrix generation, we used BUSCO v3.0.2 (Waterhouse et al. 2018) to evaluate the integrity of the Benchmarking Universal Single-Copy Orthologs assembly and extracted USCOs from the genome. The hemiptera_odb10 dataset ($n = 2,510$) was used as the reference gene set, and the reference built-in species were *Acromyrmex echinator* or *Rhodnius prolixus*. When the proportion of Fragmented USCOs in the evaluation was too large ($>20\%$), then the average USCO length parameter in the control file “length_cutoff” could be modified to restore more “complete” USCOs, so that the BUSCO pipeline could treat more fragmented USCOs as “complete” USCOs sequences. For sequence alignment, ami-

no acid sequences were aligned via MAFFT v7.450 with the L-INS-I method (Kato et al. 2019). In order to remove unreliable homologous regions, we used trimAl v1.4.1 software for trimming. In continuation, we used the scripts component in PLWS for length filtering and retained the loci with parsimony information sites greater than 95. Based on the GC content strategy and relative composition variability (RCV) strategy, we performed compositional heterogeneity detection and filtering and retained the loci with GC content less than 0.13 and RCV value less than 0.5. Finally, based on the homogeneity detection strategy, the pval value of 0.05 was input after the symmetry test of the stationarity, reversibility and homogeneity (SRH). Based on PhyKIT v1.11.10 (Steenwyk et al. 2021), the filtered sequence was combined with the obtained data using the matrix generation. sh script as written by Zhang et al. (2019) to generate a data matrix USCO80 with 80% integrity (Table 2). For the remaining loci based on alignment marker filtering, IQ-TREE v2.1.3 was used to construct a single gene tree based on the EX-EHO mixed model (Hoang et al. 2018). The bootstrap was calculated, and the average bootstraps (ABS) strategy was selected to delete the loci with weak phylogenetic signals (ABS = 50). The sequences with integrity of 80% were combined to obtain USCO80_abs50 (Table 2).

The extraction of UCEs needed to be compared with the probe set of UCEs. For groups lacking probe sets, the probe design was required before the extraction of UCEs. The probe we used was a hemiptera UCEs probe sequence (Hemiptera-UCE-2.7K-v1) as developed by Faircloth (2017). Get UCE from assembled genomes using the `UCE_extraction.sh` script in the rapid-assembly pipeline PLWS. “`phyluce_probe_run_multiple_lastzs_sqlite`”, was used to align the genome sequence with the probe sequence. “`phyluce_probe_slice_sequence_from_genomes`” was used to extract the FASTA sequence matching the UCE marker in each genome. “`phyluce_assembly_match_contigs_to_probes`” and “`phyluce_assembly_get_match_count`” were used to match the assembled contigs with the probes. “`phyluce_assembly_get_fastas_from_match_counts`” was used to extract all the successfully matched marker genes into a FASTA file. After extracting the UCE loci, the UCE matrix was constructed in a similar way to the USCO matrix. In short, by MAFFT alignment, trimAl was used to remove unreliable homologous regions, and Scripts components for length filtering to form a heterogeneity test (excluding loci with parsimony informative sites less than 100, $GC > 0.5$, $RCV > 0.25$). After the symmetry test of the SRH hypothesis, the pval value of 0.02 was input, and then the sequence was merged to generate a data matrix UCE80 with an integrity of 80%. IQ-TREE was used to construct the single gene tree of each locus based on the EX-EHO mixed model and the bootstrap was calculated. When the gene markers with high phylogenetic signal were obtained, the ABS value of 65 was input, and finally, the matrix UCE80_abs65 with integrity of 80% was generated for phylogenetic analysis. The details are shown in Table 2.

2.4. Phylogenetic analyses

We used a different set of analysis methods for phylogenetic reconstruction to minimize the impact of systematic errors in large-scale genome datasets (Sun et al. 2020). We employed the maximum likelihood (ML) and Multispecies coalescent process (MSC) model methods to construct phylogenetic trees based on different data matrices. For partition ML analysis, we used ModelFinder (Kalyaanamoorthy et al. 2017) to select the best matching surrogate model for each gene partition through the relaxed clustering algorithm ‘-rclusterf 10’ (Lanfear et al. 2014) implemented in IQ-TREE. At the same time, to reduce the computational burden, we used LG ‘-mset LG’ and GTR ‘-mset GTR’ for USCO (amino acid) and UCE (nucleotide) partition ML analysis, respectively. To solve the influence of heterogeneity on phylogenetic inference (Kolaczkowski and Thornton 2004), the general heterogeneous evolution (GHOST) model was used on a single topology to construct the ML tree, in which the selected substitution model was the LG model, and the amino acid substitution frequency model and the rate heterogeneity model between sites were set to FO and H4 models, respectively. To reduce the effects of substitution saturation and compositional heterogeneity, we used Dayhoff6 recoding (6-state amino acid recoding strategies; Hernandez and Ryan 2021): Phylogears v2.2.0 was firstly used to convert the sequence format, and then a phylogeny was inferred with IQ-TREE with “-m GTR+R” model. The rate heterogeneity model between sites was set to the R4 model. All ML analyses ran 1000 SH-aLRTs (Guindon et al. 2010) and 1000 UFBoot2 (Hoang et al. 2018). A single gene tree as generated by UCE and USCO matrices in IQ-TREE, was used to perform MSC supertree analysis on incomplete lineage sorting (ILS) using default parameters (Zhang et al. 2018) in ASTRAL-III v5.6.1.

2.5. Divergence time estimation

We use the MCMCTree in PAML v4.9j (Yang 2007) to estimate the divergence time, the Partition ML tree of the matrix USCO80_abs50 as the input tree, and the independent rate of the molecular clock. In order to avoid the falsely specified rate prior and unreasonable narrow posterior confidence interval due to the increase in the number of loci, the loci are merged into a larger partition based on the partition scheme of ML reconstruction estimation in the previous partition (Dos Reis et al. 2014; Jina and Brown 2018). The fossil records of Cicadellidae are extremely rare, and many available fossils are difficult to determine due to the lack of information on important morphological features (such as leg hairs and genitals) used for classification (Feng et al. 2024). Therefore, we calibrated the root age (113–125 million years ago, Mya) of the phylogenetic tree based on the oldest leafhopper fossil (Grimaldi 1990). Two independent runs were performed using the independent rate model, Sampfreq 5, until it collected 300,000 samples, while the first 250,000 samples were discarded as aging values.

3. Results

3.1. Genome assembly

We sequenced each sample and obtained raw data of 40 to 100 G, covering a range of 8.79 to 37.54 x. The assembled genome size ranged from 816.3 Mb (*Batracomorphus curvatus*) to 2,867.2 Mb (*Krisna viridula*), the number of Scaffolds from 213,833 to 857,534, the length of Scaffold N50 from 48.63 to 216.07 kb, the maximum read length from 59.31 to 639.44 kb, and the GC content (%) from 31.25 to 32.75. Additional statistical information (i.e., average read depth, number of stents, total length, maximum read length, and N50 length) is given in Table 1.

3.2. Matrix generation

The overall completeness (complete and single-copy/ duplicated + fragmented) of the universal single-copy ortholog extraction was 33.50–70.30% (817–1,711 sites), of which 1.00–2.70% (25–68 sites) were duplicated, and 1.10–2.60% (27–65 sites) were fragmented (Fig. 1 and Table 1). The sequence of the same point was merged into the FASTA file to obtain 2404 USCOs, which were then used for downstream analysis. After sequence alignment, screening and pruning, 2,246 loci were retained. Length filtering and composition heterogeneity detection were performed on the pruned loci, and 1,599 loci were retained. A total of 1,586 loci were obtained by the SRH test, resulting in a USCO matrix, containing 368 loci (Table 2). The average bootstraps (ABS) strategy removed loci with weak phylogenetic signals, and retained 1432 loci. Subsequently, we used 1432 loci to infer a single gene tree and then selected 358 loci with an average bootstrap value greater than 80 to generate a matrix USCO80_abs50 for phylogenetic analysis (Table 2).

After alignment and pruning, 2,416 UCE loci were retained, which were reduced to 1,901 loci by length filtering and composition heterogeneity detection. After SRH detection, it was reduced to 1,349 loci and finally reduced to 829 loci after the UCE matrix with 80% integrity (Table 2). Based on the average bootstraps (ABS) strategy, the sites with weak phylogenetic signals were deleted and reduced to 1,324 sites. Finally, 484 sites with an average value greater than 80 were selected to generate the UCE80_abs65 matrix for phylogenetic analysis (Table 2).

3.3. Phylogenetic analyses

In this study, all phylogenetic reconstructions converged on a highly consistent topology. USCO and UCE matrices yielded 5 ML trees (Figs 2, S1–S4, respectively) and 2 species trees (Figs S5, S6, respectively). A comparative analysis of phylogenetic reconstruction shows differences in the topological structure of phylogenetic trees constructed using the same model based on different USCO matrices, while the UCE matrix phylogenetic reconstruc-

Table 1. Genome assembly information of the 25 newly sequenced low-coverage whole-genomic samples.

Samples	Average read depth (x)	Assembly statistics					BUSCO (%)			
		Scaffold number	Total length (Mb)	Max read length (kb)	N50 scaffold (kb)	GC(%)	C	D	F	M
<i>Batracomorphus_cocles</i>	17.56	337823	967.75	121.62	83.29	31.87	63.80	2.00	1.80	34.40
<i>Batracomorphus_cornutus</i>	13.80	373629	995.22	229.30	91.17	32.11	59.00	2.30	1.70	39.30
<i>Batracomorphus_curvatus</i>	25.10	213833	798.17	89.45	48.63	32.72	68.50	2.00	1.50	30.00
<i>Batracomorphus_erato</i>	20.08	297978	1032.34	130.92	63.66	31.88	70.30	2.10	1.90	27.80
<i>Batracomorphus_expansus</i>	13.78	312857	834.33	112.41	75.42	31.65	60.10	1.70	2.20	37.70
<i>Batracomorphus_extentus</i>	15.06	354955	960.17	211.18	89.35	31.81	60.00	1.60	2.20	37.80
<i>Batracomorphus_furcatus</i>	25.10	367736	1238.66	210.67	86.21	32.02	33.50	1.00	1.40	65.10
<i>Batracomorphus_geminatus</i>	18.82	310638	922.38	352.83	75.82	32.05	62.70	2.70	2.00	35.30
<i>Batracomorphus_laminocus</i>	22.57	291830	896.49	166.8	70.73	32.00	65.90	1.40	2.10	32.00
<i>Batracomorphus_matsumurai</i>	20.07	239724	794.12	108.09	57.26	32.69	69.70	2.00	1.20	29.10
<i>Batracomorphus_notatus</i>	13.81	409000	906.24	208.32	112.88	31.86	57.60	1.90	1.70	40.70
<i>Batracomorphus_pandarus</i>	13.81	370876	900.13	92.63	97.01	31.81	61.30	1.80	1.70	37.00
<i>Batracomorphus_paradentatus</i>	20.07	270175	946.89	204.35	62.22	32.08	65.10	2.00	2.60	32.30
<i>Batracomorphus_strictus</i>	17.56	409213	1096.92	121.66	100.15	31.97	64.90	2.10	2.10	33.00
<i>Batracomorphus_thetis</i>	27.58	220155	804.92	240.63	50.71	32.75	68.10	2.40	1.40	30.50
<i>Batracomorphus_trifurcatus</i>	16.32	324800	904.79	213.09	77.43	31.86	63.00	1.80	2.20	34.80
<i>Gessius_rufidorsus</i>	15.02	849269	2236.87	207.40	207.05	31.26	57.30	2.00	1.60	41.10
<i>Krisna_concava</i>	12.63	752354	1535.02	190.05	216.07	31.77	44.40	1.70	1.10	54.50
<i>Krisna_furcata</i>	8.79	585163	1244.80	209.66	165.88	32.30	63.50	2.30	2.00	34.50
<i>Krisna_rufimarginata</i>	13.79	749538	1997.66	639.44	186.35	31.25	51.60	1.50	1.60	46.80
<i>Krisna_viridula</i>	13.81	857534	2712.20	211.35	177.54	31.76	51.40	2.50	1.80	46.80
<i>Trocnadella_arisana</i>	37.54	366297	1026.10	210.34	95.37	32.48	52.20	2.00	1.50	46.30
<i>Trocnadella_fasciana</i>	26.38	269856	1007.10	59.31	58.18	32.23	63.70	2.40	1.30	35.00
<i>Trocnadella_furculata</i>	20.07	313188	884.59	208.69	78.46	32.57	56.80	2.50	2.10	41.10
<i>Trocnadella_testacea</i>	25.11	294465	941.85	205.72	70.73	32.68	59.00	2.30	1.80	39.20

Table 2. Summary of USCOs (amino acid) and UCEs (nucleotide) matrices.

Matrix	Minimum taxa ration per locus (%)	Number of loci	Average missing taxa per locus (%)	Number of sites	Average locus length	Missing sites (%)
USCO80	80	368	10.79	140620	382.12	22.32
USCO80_abs50	80	358	10.82	138528	386.95	22.09
UCE80	80	829	12.83	661140	797.52	35.90
UCE80_abs65	80	484	12.90	369576	763.59	35.12

UCE, ultraconserved element; USCO, universal single-copy ortholog.

tion is concentrated on a highly consistent topology. All the results supported that the four genera involved in the study were restored to be composed of two main evolutionary branches, namely ((*Batracomorphus* + *Trocnadella*) + (*Gessius* + *Krisna*)).

In the branch (*Batracomorphus* + *Trocnadella*), *Batracomorphus* formed a large branch showing monophyly with species aggregation. This large branch divided the genus into three distinct clades with four species (*Batracomorphus cornutus*, *Batracomorphus furcatus*, *Batracomorphus geminatus* and *Batracomorphus paradentatus*), forming a small branch. In the genus *Trocnadella*, four species showed significant differences in their phylogenetic relationships as reconstructed by the two molecular markers. The phylogenetic reconstruction using the USCO matrix showed the developmental relationship as:

(((*Trocnadella arisana* + *Trocnadella testacea*) + *Trocnadella furculata*) + *Trocnadella fasciana*)); however, the reconstruction using the UCE matrix showed the developmental relationship as: (((*T. testacea* + *T. furculata*) + *T. arisana*) + *T. fasciana*)). In the (*Gessius* + *Krisna*) clade, based on the phylogenetic relationship constructed by the USCO matrix, the species involved in the genus *Krisna* were not all clustered together. Among them, *Krisna concava* and *Gessius rufidorsus* clustered into a branch to become closely related species, and *Krisna rufimarginata* formed a separate branch. *Krisna furcata* and *K. viridula* always gathered together to form a sister group. In the phylogenetic relationship constructed by the UCE matrix, *K. concava* and *K. rufimarginata* were clustered together to form closely related species with *G. rufidorsus*, *K. furcata* and *K. viridula* formed a sister group.

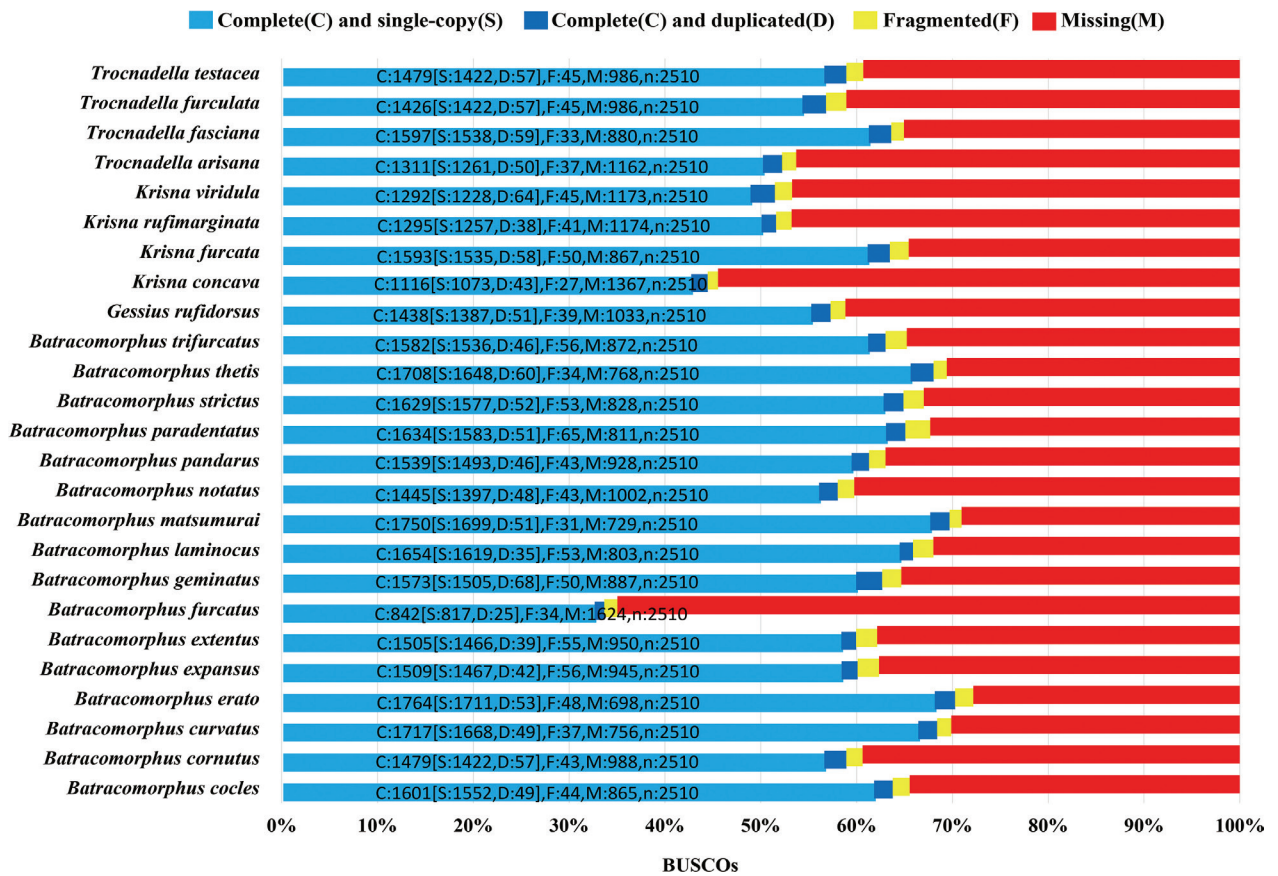


Figure 1. BUSCO genome completeness assessments: complete (C), complete single-copy (S), complete duplicated (D), fragmented (F), and missing (M).

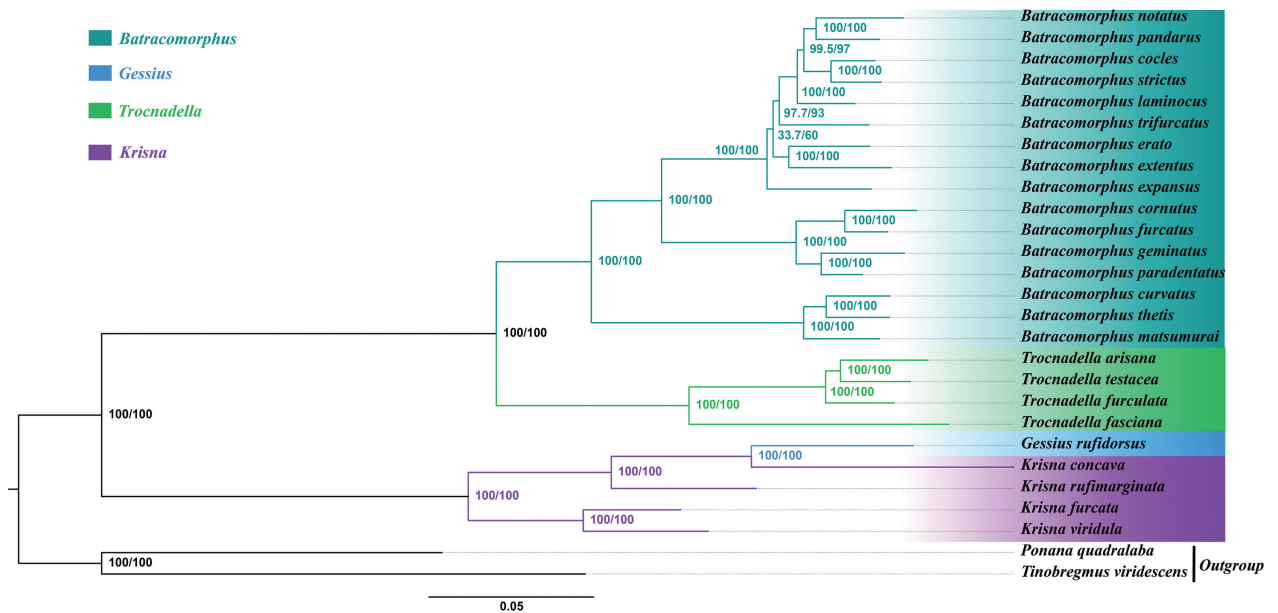


Figure 2. ML phylogenomic tree of Iassinae based on the analysis of 358 USCO loci with the Partition model in IQ-TREE. Support values on nodes indicate SH-aLRT/UFBoot2, respectively. SH-aLRT/UFBoot2 approximate values are 100/100 node values. ML, maximum likelihood; USCO, universal single-copy ortholog.

3.4. Divergence time estimation

The estimated divergence time (Fig. 3) demonstrated that the recent common ancestor divergence time of the four genera of Iassinae involved in the study was 119 Mya,

and the 95% highest posterior density (HPD) interval was 113–125 Mya, with Early Cretaceous. In the Late Cretaceous-Oligocene (26–78 Mya) stage, four genera were differentiated. The differentiation of *Batracomorphus*, *Trocnadella*, *Krisna* and *Gessius* began at 60 Mya (49–

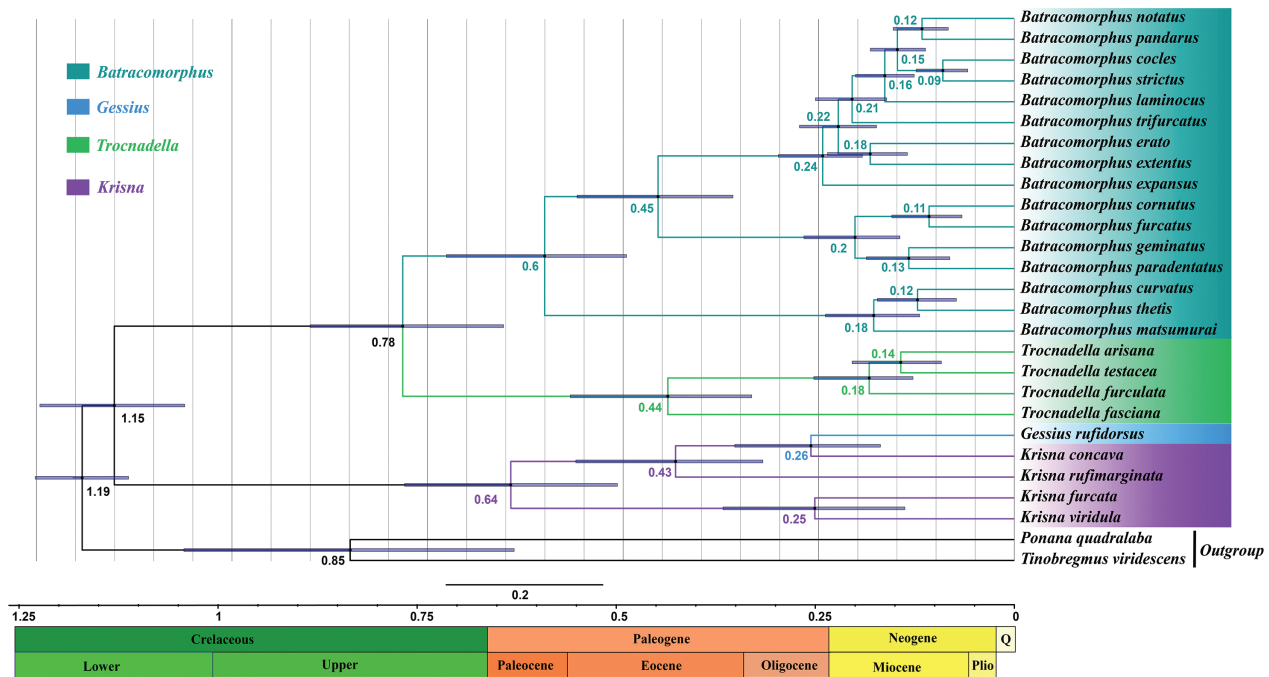


Figure 3. Divergence time estimation within Iassininae, inferred in MCMCtree on a Partition ML tree on matrix USCO80_abs50. Nodes are labeled with the age range of the most recent common ancestor, blue bar shows the 95% highest probability density interval. Q, Quaternary; Plio., Pliocene.

72 Mya, 95% HPD), 44 Mya (33–57 Mya, 95% HPD), 64 Mya (51–78 Mya, 95% HPD) and 26 Mya (17–36 Mya, 95% HPD), respectively. *Batracomorpha*, *Trocnadella*, and *Krisna* originated in the Upper Cretaceous-Eocene, and *Gessius* originated in the Eocene-Miocene.

4. Discussion

In this study, the results of BUSCO evaluation demonstrated that the integrity of our newly sequenced genome ($n = 25$) was 33.50–70.30%, which was lower than the sequencing results of Sun et al. (2020) on Collembola and Zhang et al. (2022) on 23 species of *Lasioglossum*. Based on the 25 assembled genomes, UCES were extracted. The number and extraction rate of contigs involved in UCES extraction, except for *K. concava*, only 1,194 UCES were extracted, and the number of contigs in the remaining 24 species ranged from 1,689 to 2,231. The extraction rate of UCES was 76.58–82.50%, and 1,553 to 1,782 UCES were extracted, which was higher than that of Sun et al. (2020), but lower than that of Zhang et al. (2022). The above differences may be due to the different species involved in the study and the freshness of the specimens during sequencing. In this study, the number of USCOS and UCES we obtained ranged from 817 to 1,782, which can be used to construct the phylogenetic relationship of Iassininae. The statistical analysis of the Scaffold size and N50 size assembled by 25 species showed that there were significant differences in the size between genera, but the trend of the two changes was the same, which was consistent with the standard of genome assembly. This was the

same as in the previous analysis results of insect phylogenetics based on LCWGS data (Zhang et al. 2019; Skinner 2020; Hu et al. 2022).

The topological structure of the phylogenetic tree of Iassininae based on the two molecular markers was the same. The phylogenetic relationships inferred using USCOS were slightly different, while the phylogenetic relationships constructed using UCES were completely consistent, indicating that the phylogenetic relationships constructed using UCES in Iassininae are more stable than those constructed using USCOS. The likelihood ratio test value (SH-aLRT) of the phylogenetic tree constructed by the two molecular markers was higher than the fast bootstrap value (UFBoot), and each genus had a high node support rate. Our systematic genomic analysis results supported the view of Krishnankutty et al. (2016) that Batracomorpha was established using morphological characteristics and molecular data with *Batracomorpha* as the model genus. However, they were different from Krishnankutty et al. (2016) in reconstructing the phylogenetic relationship of Iassininae based on morphological characteristics and molecular data, which may be since this study involved fewer genera and lacked foreign taxa. Phylogenetic relationships based on the two molecular markers supported the monophyletic groups of *Batracomorpha* and *Trocnadella*, which is consistent with previous phylogenetic studies (Krishnankutty et al. 2016; Wang et al. 2020). Since this study only involved one species of the *Gessius*, it is inconclusive whether it is a monophyletic or paraphyletic group. In our research, *Krisna* is a paraphyletic group, which is consistent with the results of Yang et al. (2023), and in contrast to the results of Krishnankutty et al. (2016), Wang et al. (2020), Zhang et al. (2023) and Lu et al. (2023). The reason may

be that the species involved in the study and the molecular markers used were different. By comparison, we found that the phylogenetic relationships based on USCOs and UCEs of the species involved in *Trocnadella*, *Gessius* and *Krisna* were significantly different. This phenomenon may be due to the difference in the evolutionary rate between USCOs and UCEs. Although there are differences in the phylogeny based on the two molecular markers, the results supported that *Batracomorphus* and *Trocnadella* are clustered together to form a sister group, and *Gessius* and *Krisna* also clustered together as a sister group, which is consistent with the results of Wang et al. (2020), Wang et al. (2022) and Yang et al. (2023).

The results of MCMCTree indicated that the origin of the Iassinae insects dates back to the Lower Cretaceous period, supporting the findings of Dietrich et al. (2017) and coinciding with a peak in insect diversification during the Aptian period (Schachat et al. 2019). Assessments of temporal divergence in the Evacanthinae (Wang et al. 2017) and the Sharpshooters (Feng et al. 2024) within the Cicadellinae suggested that terrestrial ecology and climate change play crucial roles in the diversification of leafhopper species. The divergence of Iassinae species also broadly aligns with the dispersal times of angiosperms (Hochuli and Feist-Burkhardt 2013; Fagua et al. 2017) and trends in surface temperature and humidity changes (Zachos et al. 2008).

Overall, based on data matrices and combinations of different models, our system's phylogenetic analysis of the Iassinae produced a generally consistent tree, where all results supported: ((*Batracomorphus* + *Trocnadella*) + (*Gessius* + *Krisna*)). Additionally, according to the MCMCTree analysis, and divergence times suggested that *Batracomorphus*, *Trocnadella* and *Krisna* originated in the late Cretaceous to Eocene, while *Gessius* diverged later, around the Eocene to Miocene. Unfortunately, our limited taxon sampling did not allow to fully elucidate the evolutionary relationships at the genus level within the Iassinae, indicating the need for further research.

5. Competing interests

The authors have declared that no competing interests exist.

6. Acknowledgments

This study thanked Feng Tian, Lan Zhang, Feng 'e Li, Min Li, Yanqiong Yang, and Xianyi Wang for their help in the collection and preservation of these insects. This study was supported by the National Natural Science Foundation of China (No. 32160119); and the Program of Excellent Innovation Talents, Guizhou Province, China (No. 20206003-2).

7. References

- Allen JM, Boyd B, Nguyen NP, Vachaspati P, Warnow T, Huang DI, Grady PGS, Bell KC, Cronk QCB, Mugisha L, Pittendrigh BR, Leonardi MS, Reed DL, Johnson KP (2017) Phylogenomics from whole genome sequences using aTRAM. *Systematic Biology* 66(5): 786–798. <https://doi.org/10.1093/sysbio/syw105>
- Blocker HD (1979) A proposed phylogeny of New World Iassinae (Homoptera: Cicadellidae). *Annals of the Entomological Society of America* 72(6): 857–862. <https://doi.org/10.1093/aesa/72.6.857>
- Bossert S, Murray EA, Almeida EA, Brady SG, Blaimer BB, Danforth BN (2019) Combining transcriptomes and ultraconserved elements to illuminate the phylogeny of Apidae. *Molecular Phylogenetics and Evolution* 130: 121–131. <https://doi.org/10.1016/j.ympev.2018.10.012>
- Branstetter MG, Müller A, Griswold TL, Orr MC, Zhu CD (2021) Ultraconserved element phylogenomics and biogeography of the agriculturally important mason bee subgenus *Osmia* (*Osmia*). *Systematic Entomology* 46(2): 453–472. <https://doi.org/10.1111/syen.12470>
- Breinholt JW, Earl C, Lemmon AR, Lemmon EM, Xiao L, Kawahara AY (2018) Resolving relationships among the megadiverse butterflies and moths with a novel pipeline for anchored phylogenomics. *Systematic Biology* 67(1): 78–93. <https://doi.org/10.1093/sysbio/syx048>
- Bushnell B (2014) BBTools. <https://sourceforge.net/projects/bbmap>
- Chen S, Zhou Y, Chen Y, Gu J (2018) fastp: an ultra-fast all-in-one FASTQ preprocessor. *Bioinformatics* 34(17): i884–i890. <https://doi.org/10.1093/bioinformatics/bty560>
- Chen T, Chen X, Zhang S, Zhu J, Tang B, Wang A, Dong L, Zhang Z, Yu C, Sun Y, Chi L, Chen H, Zhai S, Sun Y, Lan L, Zhang X, Xiao J, Bao Y, Wang Y, Zhang Z, Zhao W (2021) The genome sequence archive family: toward explosive data growth and diverse data types. *Genomics, Proteomics and Bioinformatics* 19(4): 578–583. <https://doi.org/10.1016/j.gpb.2021.08.001>
- Chikhi R, Rizk, G (2013) Space-efficient and exact de Bruijn graph representation based on a Bloom filter. *Algorithms for Molecular Biology* 8: 1–9. <https://doi.org/10.1186/1748-7188-8-22>
- CNCB-NGDC Members and Partners (2022) Database Resources of the National Genomics Data Center, China National Center for Bioinformatics in 2022. *Nucleic Acids Research* 50(D1): D27–D38. <https://doi.org/10.1093/nar/gkab951>
- Dai W, Dietrich CH, Zhang Y (2015) A review of the leafhopper tribe Hyalojassini (Hemiptera: Cicadellidae: Iassinae) with description of new taxa. *Zootaxa* 3911(1): 1–42. <http://dx.doi.org/10.11646/zootaxa.3911.1.1>
- Dietrich CH (1999) The role of grasslands in the diversification of leafhoppers (Homoptera: Cicadellidae): a phylogenetic perspective. In *Proceedings of the Fifteenth North American Prairie Conference*, Bend: Natural Areas Association, 44–49.
- Dietrich CH (2005) Keys to the families of Cicadomorpha and subfamilies and tribes of Cicadellidae (Hemiptera: Auchenorrhyncha). *Florida Entomologist* 88(4): 502–517. [https://doi.org/10.1653/0015-4040\(2005\)88\[502:KTTFOC\]2.0.CO;2](https://doi.org/10.1653/0015-4040(2005)88[502:KTTFOC]2.0.CO;2)
- Dietrich CH, Allen JM, Lemmon AR, Moriarty LE, Takiya DM, Evangelista O, Walden KKO, Grady PGS, Johnson KP (2017) Anchored hybrid enrichment-based phylogenomics of leafhoppers and treehoppers (Hemiptera: Cicadomorpha: Membracoidea). *Insect Systematics and Diversity* 1(1): 57–72. <https://doi.org/10.1093/isd/ixx003>
- Dietrich CH, Rakitov RA, Holmes JL, Black IV WC (2001) Phylogeny of the major lineages of Membracoidea (Insecta: Hemiptera: Cicadomorpha) based on 28S rDNA sequences. *Molecular Phylogenetics and Evolution* 18(2): 293–305. <https://doi.org/10.1006/mpev.2000.0873>
- Domahovski AC (2019) New genera and species of Selenomorphini (Hemiptera: Cicadellidae: Iassinae), including redescription of Sca-

- roidana Osborn, Pachyopsis Uhler and updated key to genera and species. *Zootaxa* 4711(3): 517–544. <https://doi.org/10.11646/zootaxa.4711.3.5>
- Domahovski AC, Cavichioli RR (2023) Phylogenetic analysis and revision of the leafhopper genus *Acuera* DeLong & Freytag (Hemiptera: Cicadellidae: Gyponini) based on morphological data. *Arthropod Systematics & Phylogeny* 81: 79–164. <https://doi.org/10.3897/asp.81.e81961>
- Dos Reis M, Zhu T, Yang Z (2014) The impact of the rate prior on Bayesian estimation of divergence times with multiple loci. *Systematic Biology* 63(4): 555–565. <https://doi.org/10.1093/sysbio/syu020>
- Fagua G, Condamine FL, Horak M, Zwick A, Sperling FA (2017) Diversification shifts in leafroller moths linked to continental colonization and the rise of angiosperms. *Cladistics* 33(5): 449–466. <https://doi.org/10.1111/cla.12185>
- Faircloth BC (2017) Identifying conserved genomic elements and designing universal bait sets to enrich them. *Methods in Ecology and Evolution* 8(9): 1103–1112. <https://doi.org/10.1111/2041-210X.12754>
- Feng L, Takiya DM, Krishnankutty SM, Dietrich CH, Zhang Y (2024) Phylogeny and biogeography of the sharpshooters (Hemiptera: Cicadellidae: Cicadellinae). *Systematic Entomology* 49(2): 314–329. <https://doi.org/10.1111/syen.12620>
- Grimaldi DA (Ed.) (1990) *Insects from the Santana Formation, lower cretaceous, of Brazil*. New York: American Museum of Natural History, 1–191pp.
- Guindon S, Dufayard JF, Lefort V, Anisimova M, Hordijk W, Gascuel O (2010) New algorithms and methods to estimate maximum-likelihood phylogenies: assessing the performance of PhyML 3.0. *Systematic Biology* 59(3): 307–321. <https://doi.org/10.1093/sysbio/syq010>
- Hernandez AM, Ryan JF (2021) Six-state amino acid recoding is not an effective strategy to offset compositional heterogeneity and saturation in phylogenetic analyses. *Systematic Biology* 70(6): 1200–1212. <https://doi.org/10.1101/729103>
- Hoang DT, Chernomor O, Von Haeseler A, Minh BQ, Vinh LS (2018) UFBoot2: improving the ultrafast bootstrap approximation. *Molecular Biology and Evolution* 35(2): 518–522. <https://doi.org/10.1093/molbev/msx281>
- Hochuli PA, Feist-Burkhardt S (2013) Angiosperm-like pollen and Afropollis from the Middle Triassic (Anisian) of the Germanic Basin (northern Switzerland). *Frontiers in Plant Science* 4: 344. <https://doi.org/10.3389/fpls.2013.00344>
- Hu Y, Dietrich CH, Skinner RK, Zhang Y (2022) Phylogeny of Membracoidea (Hemiptera: Auchenorrhyncha) based on transcriptome data. *Systematic Entomology* 48(1): 97–110. <https://doi.org/10.1111/syen.12563>
- Jin Y, Brown RP (2018) Partition number, rate priors and unreliable divergence times in Bayesian phylogenetic dating. *Cladistics* 34(5): 568–573. <https://doi.org/10.1111/cla.12223>
- Kalyaanamoorthy S, Minh BQ, Wong TK, Von Haeseler A, Jermiin LS (2017). ModelFinder: fast model selection for accurate phylogenetic estimates. *Nature Methods* 14(6): 587–589. <https://doi.org/10.1038/nmeth.4285>
- Kapli P, Yang Z, Telford MJ (2020) Phylogenetic tree building in the genomic age. *Nature Reviews Genetics* 21(7): 428–444. <https://doi.org/10.1038/s41576-020-0233-0>
- Katoh K, Rozewicki J, Yamada KD (2019) MAFFT online service: multiple sequence alignment, interactive sequence choice and visualization. *Briefings in Bioinformatics* 20(4): 1160–1166. <https://doi.org/10.1093/bib/bbx108>
- Kolaczkowski B, Thornton JW (2004) Performance of maximum parsimony and likelihood phylogenetics when evolution is heterogeneous. *Nature* 431(7011): 980–984. <https://doi.org/10.1038/nature02917>
- Krishnankutty SM, Dietrich CH, Dai W, Siddappaji MH (2016) Phylogeny and historical biogeography of leafhopper subfamily Iassinae (Hemiptera: Cicadellidae) with a revised tribal classification based on morphological and molecular data. *Systematic Entomology* 41(3): 580–595. <https://doi.org/10.1111/syen.12175>
- Lanfear R, Calcott B, Kainer D, Mayer C, Stamatakis A (2014) Selecting optimal partitioning schemes for phylogenomic datasets. *BMC Evolutionary Biology* 14: 1–14. <https://doi.org/10.1186/1471-2148-14-82>
- Lei M, Dong D (2016) Phylogenomic analyses of bat subordinal relationships based on transcriptome data. *Scientific Reports* 6(1): 27726. <https://doi.org/10.1038/srep27726>
- Lemmon AR, Emme SA, Lemmon EM (2012). Anchored hybrid enrichment for massively high-throughput phylogenomics. *Systematic Biology* 61(5): 727–744. <https://doi.org/10.1093/sysbio/sys049>
- Lemmon EM, Lemmon AR (2013) High-throughput genomic data in systematics and phylogenetics. *Annual Review of Ecology, Evolution, and Systematics* 44(1): 99–121. <https://doi.org/10.1146/annurev-ecolsys-110512-135822>
- Leo C, Carapelli A, Cicconardi F, Frati F, Nardi F (2019) Mitochondrial genome diversity in Collembola: phylogeny, dating and gene order. *Diversity* 11(9): 169. <https://doi.org/10.3390/d11090169>
- Li H (2018) Minimap2: pairwise alignment for nucleotide sequences. *Bioinformatics* 34(18): 3094–3100. <https://doi.org/10.1093/bioinformatics/bty191>
- Li H, Handsaker B, Wysoker A, Fennell T, Ruan J, Homer N, Marth G, Abecasis G, Durbin R (2009) The sequence alignment/map format and SAMtools. *Bioinformatics* 25(16): 2078–2079. <https://doi.org/10.1093/bioinformatics/btp352>
- Lu J, Wang J, Li D, Wang X, Dai R (2023). Description of the whole mitochondrial genome of *Bhatia longiradiata* (Hemiptera, Cicadellidae, Deltocephalinae: Drabescini) and phylogenetic relationship. *Genes & Genomics* 45(1): 59–70. <https://doi.org/10.1007/s13258-022-01338-6>
- Luo R, Li, B, Xie Y, Li Z, Huang W, Yuan J, He G, Chen Y, Pan Q, Liu Y, Tang J, Wu G, Zhang H, Shi Y, Liu Y, Yu C, Wang B, Lu Y, Han C, Cheung DW, Yiu S, Peng S, Zhu X, Liu G, Liao X, Li Y, Yang H, Wang J, Lam TK, Wang J (2012) SOAPdenovo2: an empirically improved memory-efficient short-read de novo assembler. *Gigascience* 1(1): 2047–217X. <https://doi.org/10.1186/2047-217X-1-18>
- Ma ZY, Nie ZL, Liu XQ, Tian JP, Zhou YF, Zimmer E, Wen J (2023) Phylogenetic relationships, hybridization events, and drivers of diversification of East Asian wild grapes as revealed by phylogenomic analyses. *Journal of Systematics and Evolution* 61(2): 273–283. <https://doi.org/10.1111/jse.12918>
- Ozsolak F, Milos PM (2011) RNA sequencing: advances, challenges and opportunities. *Nature Reviews Genetics* 12(2): 87–98. <https://doi.org/10.1038/nrg2934>
- Peters RS, Krogmann L, Mayer C, Donath A, Gunkel S, Meusemann K, Kozlov A, Podsiadlowski L, Petersen M, Lanfear R, Diez PA, Heraty J, Kjer KM, Klopstein S, Meier R, Polidori C, Schmitt T, Liu S, Zhou X, Wappler T, Rust J, Misof B, Niehuis O (2017) Evolutionary history of the Hymenoptera. *Current Biology* 27(7): 1013–1018. <https://doi.org/10.1016/j.cub.2017.01.027>

- Pryszcz LP, Gabaldón T (2016) Redundans: an assembly pipeline for highly heterozygous genomes. *Nucleic Acids Research* 44(12): e113–e113. <https://doi.org/10.1093/nar/gkw294>
- Sahlin K, Vezzi F, Nystedt B, Lundeberg J, Arvestad L (2014) BESST-efficient scaffolding of large fragmented assemblies. *BMC Bioinformatics* 15: 1–11. <https://doi.org/10.1186/1471-2105-15-281>
- Schachat SR, Labandeira CC, Clapham ME, Payne JL (2019) A Cretaceous peak in family-level insect diversity estimated with mark-recapture methodology. *Proceedings of the Royal Society B* 286(1917): 2019–2054. <https://doi.org/10.1098/rspb.2019.2054>
- Skinner RK, Dietrich CH, Walden KK, Gordon E, Sweet AD, Podsiadlowski L, Petersen M, Simon C, Takiya DM, Johnson KP (2020) Phylogenomics of Auchenorrhyncha (Insecta: Hemiptera) using transcriptomes: examining controversial relationships via degeneracy coding and interrogation of gene conflict. *Systematic Entomology* 45(1): 85–113. <https://doi.org/10.1111/syen.12381>
- Steenwyk JL, Buida III TJ, Labella AL, Li Y, Shen XX, Rokas A (2021) PhyKIT: a broadly applicable UNIX shell toolkit for processing and analyzing phylogenomic data. *Bioinformatics* 37(16): 2325–2331. <https://doi.org/10.1093/bioinformatics/btab096>
- Sun X, Ding Y, Orr MC, Zhang F (2020) Streamlining universal single-copy orthologue and ultraconserved element design: A case study in Collembola. *Molecular ecology resources* 20(3): 706–717. <https://doi.org/10.1111/1755-0998.13146>
- Wang J, Wu Y, Dai R, Yang M (2020) Comparative mitogenomes of six species in the subfamily Iassinae (Hemiptera: Cicadellidae) and phylogenetic analysis. *International Journal of Biological Macromolecules* 149: 1294–1303. <https://doi.org/10.1016/j.ijbiomac.2020.01.270>
- Wang XY, Li DF, Li H, Wang JJ, Li YJ, Dai RH (2022) Comparison of mitogenomes of three Petalocephala species (Hemiptera: Cicadellidae: Ledrinae) and their phylogenetic analysis. *Archives of Insect Biochemistry and Physiology* 111(1): e21902. <https://doi.org/10.1002/arch.21902>
- Wang Y, Dietrich CH, Zhang Y (2017) Phylogeny and historical biogeography of leafhopper subfamily Evacanthinae (Hemiptera: Cicadellidae) based on morphological and molecular data. *Scientific Reports* 7(1): 45387. <https://doi.org/10.1038/srep45387>
- Waterhouse RM, Seppey M, Simão FA, Manni M, Ioannidis P, Kliuchnikov G, Kriventseva, EV, Zdobnov EM (2018) BUSCO applications from quality assessments to gene prediction and phylogenomics. *Molecular Biology and Evolution* 35(3): 543–548. <https://doi.org/10.1093/molbev/msx319>
- Williams TA, Cox CJ, Foster PG, Szöllösi GJ, Embley TM (2020) Phylogenomics provides robust support for a two-domains tree of life. *Nature ecology & evolution* 4(1): 138–147. <https://doi.org/10.1038/s41559-019-1040-x>
- Wong D, Norman H, Creedy TJ, Jordaens K, Moran KM, Young A, Mengual X, Skevington JH, Vogler AP (2023) The phylogeny and evolutionary ecology of hoverflies (Diptera: Syrphidae) inferred from mitochondrial genomes. *Molecular Phylogenetics and Evolution* 184: 107759. <https://doi.org/10.1016/j.ympev.2023.107759>
- Yang Y, Wang J, Dai R, Wang X (2023) Structural characteristics and phylogenetic analysis of the mitochondrial genomes of four Krishna species (Hemiptera: Cicadellidae: Iassinae). *Genes* 14(6): 1175. <https://doi.org/10.3390/genes14061175>
- Yang Z (2007) PAML 4: phylogenetic analysis by maximum likelihood. *Molecular Biology and Evolution* 24(8): 1586–1591. <https://doi.org/10.1093/molbev/msm088>
- Young AD, Gillung JP (2020) Phylogenomics—principles, opportunities and pitfalls of big-data phylogenetics. *Systematic entomology* 45(2): 225–247. <https://doi.org/10.1111/syen.12406>
- Zachos JC, Dickens GR, Zeebe RE (2008) An early Cenozoic perspective on greenhouse warming and carbon-cycle dynamics. *Nature* 451(7176): 279–283. <https://doi.org/10.1038/nature06588>
- Zhang C, Rabiee M, Sayyari E, Mirarab S (2018) ASTRAL-III: polynomial time species tree reconstruction from partially resolved gene trees. *BMC Bioinformatics* 19: 15–30. <https://doi.org/10.1186/s12859-018-2129-y>
- Zhang D, Niu ZQ, Luo AR, Orr MC, Ferrari RR, Jin JF, Wu QT, Zhang F, Zhu CD (2022) Testing the systematic status of Homalictus and Rostrohalictus with weakened cross-vein groups within Halictini (Hymenoptera: Halictidae) using low-coverage whole-genome sequencing. *Insect Science* 29(6): 1819–1833. <https://doi.org/10.1111/1744-7917.13034>
- Zhang F, Ding Y, Zhu CD, Zhou X, Orr MC, Scheu S, Luan YX (2019) Phylogenomics from low-coverage whole-genome sequencing. *Methods in Ecology and Evolution* 10(4): 507–517. <https://doi.org/10.1111/2041-210x.13145>
- Zhang N, Pu T, Wang J, Tan W, Yuan Z, Li C, Song Y (2023) Phylogenetic Analysis of Two New Mitochondrial Genomes of *Singapore shinshana* and *Seriana bacilla* from the Karst Region of Southwest China. *Genes* 14(7): 1318. <https://doi.org/10.3390/genes14071318>

Supplementary Material 1

Figures S1–S6

Authors: Lu X, Lu J, Wu F, Guo S, Smagghe G, Dai R (2025)

Data type: .pdf

Explanation notes: **Figure S1.** ML phylogenomic tree of Iassinae based on the analysis of 358 USCO loci with the GHOST model in IQ-TREE. Node values represent SH-aLRT/UFBoot2, respectively. — **Figure S2.** ML phylogenomic tree of Iassinae based on the analysis of 358 USCO loci with the Dayhoff6 recording mode in IQ-TREE. Node values represent SH-aLRT/UFBoot2, respectively. — **Figure S3.** ML phylogenomic tree of Iassinae based on the analysis of 484 UCE loci with the Partition model in IQ-TREE. Node values represent SH-aLRT/UFBoot2, respectively. — **Figure S4.** ML phylogenomic tree of Iassinae based on the analysis of 484 UCE loci with the GHOST model in IQ-TREE. Node values represent SH-aLRT/UFBoot2, respectively. — **Figure S5.** MSC supertree of Iassinae based on the analysis of 368 USCO loci in ASTRAL. Node values represent local posterior probability. — **Figure S6.** MSC supertree of Iassinae based on the analysis of 829 UCE loci in ASTRAL. Node values represent local posterior probability.

Copyright notice: This dataset is made available under the Open Database License (<http://opendatacommons.org/licenses/odbl/1.0>). The Open Database License (ODbL) is a license agreement intended to allow users to freely share, modify, and use this dataset while maintaining this same freedom for others, provided that the original source and author(s) are credited.

Link: <https://doi.org/10.3897/asp.83.e142332.suppl1>